

Ceria/Polymer Hybrid Nanoparticles as Efficient Catalysts for the Hydration of Nitriles to Amides

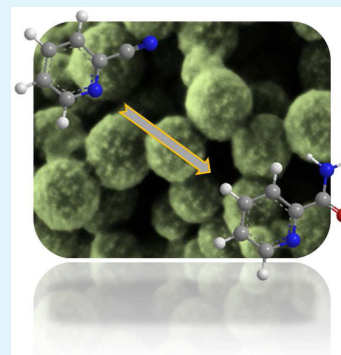
Margherita Mari, Beate Müller, Katharina Landfester, and Rafael Muñoz-Espí*

Max Planck Institute for Polymer Research, Ackermannweg 10, 55128 Mainz, Germany

S Supporting Information

ABSTRACT: We report the synthesis of ceria/polymer hybrid nanoparticles and their use as effective supported catalysts for the hydration of nitriles to amide, exemplified with the conversion of 2-cyanopyridine to 2-picolinamide. The polymeric cores, made of either polystyrene (PS) or poly(methyl methacrylate) (PMMA), are prepared by miniemulsion copolymerization in the presence of different functional comonomers that provide carboxylic or phosphate groups: acrylic acid, maleic acid, and ethylene glycol methacrylate phosphate. The functional groups of the comonomers generate a corona around the main polymer particle and serve as nucleating agents for the in situ crystallization of cerium(IV) oxide. The obtained hybrid nanoparticles can be easily redispersed in water or ethanol. The conversion of amides to nitriles was quantitative for most of the catalytic samples, with yields close to 100%. According to our experimental observations by high-performance liquid chromatography (HPLC), no work up is needed to separate the product from unreacted substrate. The substrate remains absorbed on the catalyst surface, whereas the product can be easily separated. The catalysts are shown to be recyclable and can be reused for a large number of cycles without loss in efficiency.

KEYWORDS: miniemulsion, organic–inorganic, nanoparticles, ceria, catalysis, hydration



INTRODUCTION

Well-known for their excellent catalytic properties, metal oxides are also known for having certain limitations, such as the tendency to aggregate, a difficult dispersibility/redispersibility in different solvents, and weak mechanical strength.¹ An increasingly used strategy to overcome these limitations is the combination of the metal oxide nanoparticles with polymers to produce polymer/inorganic hybrid materials, which are able to combine features of both types of materials to yield products with enhanced properties.

Hybrid nanoparticles represent a particular case of hybrid materials with very high potential in catalysis. Several approaches to obtain hybrid nanoparticles have been studied in the past few years, employing organic additives or polymer templates and involving often the use of low molecular or copolymeric surfactants as main actors in the interfacial chemistry between the organic and inorganic components.^{2,3} In the past, long polyelectrolyte chains were grown on the surface of polymer particles and their behavior in the presence of salts to obtain noble metals was extensively investigated.^{4–9} This type of approach was also extended to the immobilization of TiO₂ on polystyrene particles functionalized with sodium sulfonate brushes.¹⁰ By using different synthetic pathways, in situ deposition on polymer particles has also been reported for other metal oxides, hydroxides, and chalcogenides, including ZnO,^{11,12} Fe₂O₃ and Fe₃O₄,¹² CeO₂,¹² In(OH)₃,¹³ ZnS,¹⁴ or CdS.¹⁵

In the literature, there are few examples of polymer-supported cerium(IV) oxide (or ceria, CeO₂) in which the

hybrid particles are prepared starting from nanosized metal oxide formed *ex situ*¹⁶ or crystallized by hydrothermal method on electrospun cellulose fibers.¹⁷ Our group showed recently that ceria can be crystallized in a controlled manner on the surface of polymer nanoparticles functionalized by miniemulsion copolymerization with surface-active functional comonomers (i.e., so-called “surfmers”, monomers that act simultaneously as a surfactant, without need of further stabilization of the droplets).¹² Although surfmers allow for a precise surface functionalization and crystallization, their synthesis may be time-demanding, which limits the scaling up the process for practical applications. On the contrary, the approach reported here is a “one-pot” process that could be easily scaled up.

Cerium oxide is a well-known catalyst, mainly due to the redox activity of the couple Ce(IV)/Ce(III), with a change from one oxidation state to the other depending on the reaction conditions.¹⁸ The oxidation of CO is one of the reactions in which CeO₂ catalysts are most commonly used, followed by the oxidation of hydrocarbons. In both cases, CO₂ is the main product, making ceria a very useful catalyst to reduce the amount of pollutant from exhaust. For this field of applications, ceria is often supported on alumina,^{19–21} silica,^{22–24} active carbon,²⁵ and occasionally on zeolite.²⁶ CeO₂ finds also applications in many other reactions. The interesting acid–base properties in combination with the redox

Received: August 26, 2014

Accepted: May 6, 2015

Published: May 6, 2015

behavior allow ceria to catalyze a wide range of organic reactions, including those preferentially catalyzed on acid–base sites (i.e., dehydration^{27,28} and ketonization^{29,30}), those preferentially catalyzed by redox centers (i.e., reduction and oxidation of organic compounds³¹), and those requiring both acid–base and redox sites (i.e., addition,^{32–34} substitution, isomerization, and ring opening³⁵). Typically, an efficient activity of ceria requires a calcination step to ensure the complete conversion of cerium hydroxides, and also quite high reaction temperatures (150–400 °C).

As a model catalytic reaction with significant industrial importance, we consider here the hydration of nitriles to amides. Traditional methods involve the use of strong acid or base catalysts, which has as drawbacks the over hydrolysis of amides into carboxylic acids and the formation of salts after neutralization of the catalysts. Different types of catalysts have been tested, including both homogeneous (e.g., Pt(II),³⁶ Ru(II),³⁷ Co(III),³⁸ and Mo(IV)³⁹ complexes) and heterogeneous (e.g., Ru(OH)₃ supported on alumina⁴⁰ and MnO₂⁴¹). CeO₂ has also been shown to act as a selective heterogeneous catalyst for the hydration of nitriles that have a heteroatom (N or O) adjacent to the α carbon of the CN group.⁴²

In the present work, we present a synthetic pathway to have a ceria catalyst in a water medium, supported on polymer nanoparticles, easily redispersible in polar media and easily recoverable by centrifugation, without the requirement of any calcination step. The approach is much simpler than previously reported work, as the original polymer particles are simply functionalized with commercially available comonomers. We show how the colloidally stable ceria/polymer hybrid nanoparticles can act as efficient catalysts for the hydration of nitriles in aqueous media.

■ EXPERIMENTAL SECTION

Chemicals. Methyl methacrylate (MMA, 99%, Merck) and styrene (99%, Fluka) were passed through an aluminum oxide column before use for removal of the stabilizer. Acrylic acid (AA, 99%, Fluka), maleic acid (MA, 99%, Sigma-Aldrich), ethylene glycol methacrylate phosphate (EGMP, 99% Sigma-Aldrich), sodium dodecyl sulfate (SDS, 99%, Roth), Lutensol AT 50 (99%, BASF, a poly(ethylene oxide)-hexadecyl ether with an ethylene oxide block length of about 50 units, BASF), 2,2'-azobis(2-methylbutyronitrile) (AMBN, 99%, Wako Pure Chemical Industries), Ce(NO₃)₃·6H₂O (99%, Fluka), and NaOH (99%, Riedel-de-Haën), ethanol (analytical grade, Fisher Scientific), and 2-cyanopyridine (99%, Sigma-Aldrich) were used as received.

Synthesis of Functionalized Polymer Nanoparticles. The oil phase was prepared by stirring the main monomer (MMA or styrene, 5.76 g), hexadecane (250 mg), and AMBN (100 mg) for 30 min. The aqueous phase was prepared by dissolving the surfactant, either Lutensol AT 50 (500 mg) or SDS (100 mg), and the functional comonomer (AA, MA or EGMP, 0.24 g) in water (24 g). The oil and the water phases were mixed and pre-emulsified by stirring for 1 h. Afterward, the mixture was ultrasonified for 2 min (Branson Sonifier W-450D, 1/2-in. tip, 90% amplitude, 1.0 s pulse, 0.1 s pause), while cooling in an ice–water bath to avoid polymerization due to heating. The polymerization reaction took place in a closed round flask placed in an oil bath at 72 °C under stirring for 16–18 h. The size of the particles was characterized by dynamic light scattering (DLS) measurements at 90° (Submicron Particle Sizer NICOMP 380), and the surface charge density was determined by so-called polyelectrolyte titration (Metrohm 702 SM Titrino), that is, by titrating the negative charges with an aqueous solution of the oppositely charged polyelectrolyte poly(diallyldimethylammonium chloride).⁴³

The particle dispersions were purified by “centrifugation dialysis” with Amicon Ultra-4 centrifuge tubes (30k MWCO) according to the

following procedure: 500 μ L of latex and 500 μ L of water were placed in the upper section of the tube and 6.5 mL of water in the lower part. The tubes were centrifuged three times at 4000 rpm for 30 min, changing each time the water in the lower part of the tube and adding 500 μ L of additional pure water in the upper section. The dialyzed latex was transferred in a vial and diluted with water to reach a total volume of 20 mL.

Crystallization of Ceria on Polymer Nanoparticles. For the metal oxide formation, a dispersion amount corresponding to 30 mg of dry particles were diluted in 25 mL of an aqueous solution containing Ce(NO₃)₃ (65 mg). The oxide precipitation was conducted by dropping 5 mL of a 30 mM NaOH aqueous solution, dropped at a rate of 5 mL/h and stirred for 16–18 h. The resulting hybrid particles were characterized by scanning electron microscopy (LEO 1530 Gemini) and transmission electron microscopy (Jeol 1400). X-ray diffraction (XRD) patterns of powder samples dried under vacuum at 40 °C were recorded in a Philips PW 1820 diffractometer using CuK α radiation (λ = 1.5418 Å). The inorganic content of the samples was determined by thermogravimetric analysis (Mettler Toledo TGA-851, heating rate: 10 °C/min) and the surface area was determined by nitrogen absorption at 100 °C according to a Brunauer–Emmett–Teller (BET) isotherm in a Quantachrome Autosorb-1 equipment.

Catalysis Experiments (Hydration of Cyanopyridine). Each sample was weighted in a round flask to have a content of 20 mg of CeO₂, taking into account the inorganic content of the hybrid particles estimated by thermogravimetric analysis (TGA). The particles were stirred with a 1:1 H₂O/ethanol mixture (2 mL) until a good redispersion was achieved. After addition of 2-cyanopyridine (135 mg, 1.3 mmol), the reaction flask was heated at 80 °C for 16 h. Afterward, the particles were washed and centrifuged three times with ethanol. The product was collected and dried under vacuum at room temperature, and the yield measured by high-performance liquid chromatography (HPLC) by using an Agilent Series 1200 chromatograph equipped with a Quaternary Pump Series 1100 and a photodiode array detector (DAD) set at a wavelength of 260 nm. The chromatography was conducted with a RP-Phase Macherey-Nagel HD18 column (length, 125 mm; diameter, 4 mm; particle size, 5 μ m) running at 20 °C with a flow of 1 mL/min. The amount of injected samples was always 4 μ L, eluted by a gradient of tetrahydrofuran/(water + 0.01% trifluoroacetic acid) starting at 2/98% up to 100% of tetrahydrofuran in 10 min.

For the study of the kinetics, 100 μ L aliquots were taken from the reaction bulk after 0.25, 0.5, 1, 2, 4, 6, 8, and 24 h. Each sample was washed three times with ethanol and centrifuged to separate the catalyst (i.e., the hybrid particles). Finally, the extracted product was dried and the yield was obtained by HPLC analysis under the conditions described above.

■ RESULTS AND DISCUSSION

Surface-functionalized polymer nanoparticles, comprising a core of either polystyrene (PS) or poly(methyl methacrylate) (PMMA) and a functional corona of carboxylic or phosphate groups, were first synthesized by miniemulsion copolymerization. Afterward, cerium(IV) oxide (Ce₂O) nanoparticles were crystallized in situ on the surface of the polymer particles by following a procedure previously reported by our group.¹² Figure 1 depicts schematically the preparation of the ceria/polymer hybrid nanoparticles. Differently from unsupported ceria nanoparticles, our supported catalysts (i.e., ceria crystallized on the surface of polymer particles) are homogeneously dispersed in the aqueous suspension and can be very easily separated after the catalyzed reaction has finished.

1. Synthesis of Ceria/Polymer Hybrid Nanoparticles. Acrylic acid (AA), maleic acid (MA), or ethylene glycol methacrylate phosphate (EGMP) were chosen as functional comonomers to provide a negative charged functionalization to the surface of the particles. Two different surfactants were

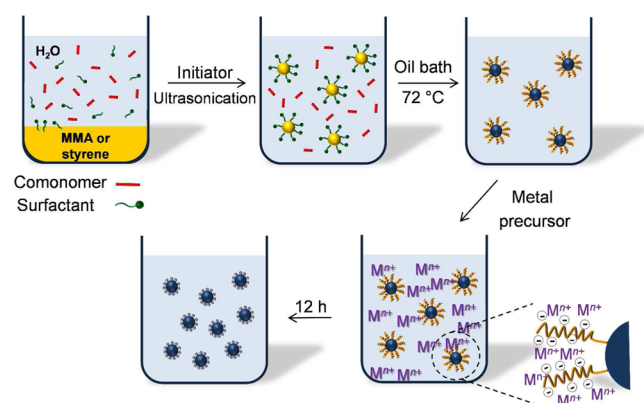


Figure 1. Schematic representation of the preparation of ceria/polymer hybrid nanoparticles by miniemulsion polymerization followed by in situ crystallization on the particle surface.

employed to stabilize the nanodroplets: an ionic surfactant (sodium dodecyl sulfate, SDS) and a poly(ethylene oxide)-based nonionic one (Lutensol AT 50). By using surfactants of different nature, we aimed to have a complete study of the system and an evaluation of how the ionic or nonionic character of the surfactant can affect the efficiency of the in situ crystallization.

The hydrophilic groups of the functional comonomers tend to be placed at the interface and exposed to the water phase. The latex corona is comprised of the hydrophilic component of the surfactant (either the sulfate groups of SDS or the poly(ethylene oxide) segments of Lutensol AT 50) and hydrophilic segments of the copolymer formed between styrene or MMA and the hydrophilic functional comonomer. A certain concentration of hydrophilic groups will be present at the surface of the particles.

The main difference between the resulting particles is the surface charge density (Table 1), with higher values of charged groups per surface area for SDS-stabilized particles, in coherence with the ionic nature of the surfactant. As a general trend, the presence of the three comonomers exhibit, as

expected, an increased number of charged groups. The only rather anomalous low values were those obtained for latexes prepared by copolymerization of MMA with maleic acid and with EGMP in the presence of the surfactant Lutensol AT 50. The low surface charge density and the low stability of these latex samples suggest a nonefficient copolymerization between MMA and the two comonomers under the synthesis conditions.

Regarding the particles size, SDS-stabilized particles are in a range of 80 to 140 nm, whereas those prepared with Lutensol AT 50 are slightly bigger, ranging from 140 to 220 nm (Table 1).

2. Formation of Metal Oxide on the Nanoparticle Surface. The formation of metal oxides on the surface of functionalized nanoparticles requires in the first place an accurate removal of surfactant, monomer and oligomer molecules that are not strongly bound to the surface. This purification step is necessary to avoid weak interactions between cerium(IV) oxide and the particle surface leading to the loss of inorganic crystals, which would reduce the efficiency of the surface crystallization.

The process started by adding the metal salt precursor to the latex dispersion for complexation of the metal ions to the functional groups of the oligomeric hydrophilic chains (cf. Figure 1). After a sufficient interaction time, the precipitating agent was dropped at a controlled rate under stirring to ensure the complete crystallization of the metal oxide in the form of small crystallites at the particle surface. The amount of inorganic content, determined by thermogravimetric analysis (TGA), ranged between 20 and 30% for all samples (Table 1). Nitrogen adsorption measurements, using the Brunauer–Emmett–Teller (BET) model, gave values of specific surface area between 12 and 18 m²/g for the pure polymer particles and 29–30 m²/g for the hybrid particles after crystallization of ceria.

Similar morphological features were confirmed for all samples by electron microscopy (Supporting Information, Figures S1 and S2). Scanning and transmission electron micrographs of two representative samples, namely poly-

Table 1. Characteristics of the Catalytic Ceria/Polymer Hybrid Particles Prepared in This Work, Together with the Product Yield Obtained in Their Presence for the Conversion of 2-Cyanopyridine to 2-Picolinamide (Last Column)

sample no.	copolymers ^a	surfactant	diameter (nm) ^b	surface charge density (charged groups/nm ²) ^c	inorganic content (%) ^d	product yield (%)
1	S	Lut. AT 50	140 ± 40	0.08 ± 0.01	0.0	
2	S	SDS	100 ± 20	0.66 ± 0.02	0.0	
3	S/AA	Lut. AT 50	140 ± 20	2.62 ± 0.04	22.8	99.9
4	S/AA	SDS	90 ± 25	1.22 ± 0.01	21.6	99.9
5	S/MA	Lut. AT 50	140 ± 20	1.04 ± 0.03	31.4	99.9
6	S/MA	SDS	130 ± 30	2.08 ± 0.03	21.2	99.9
7	S/EGMP	Lut. AT 50	140 ± 10	2.83 ± 0.06	27.2	99.1
8	S/EGMP	SDS	130 ± 10	1.34 ± 0.03	22.5	99.9
9	MMA	Lut. AT 50	220 ± 60	0.24 ± 0.01	0.0	
10	MMA	SDS	80 ± 30	0.71 ± 0.01	0.0	
11	MMA/AA	Lut. AT 50	180 ± 50	1.94 ± 0.02	27.0	95
12	MMA/AA	SDS	140 ± 20	2.65 ± 0.02	21.4	96.9
13	MMA/MA	Lut. AT 50	140 ± 40	0.64 ± 0.02	26.5	87.1
14	MMA/MA	SDS	140 ± 40	1.84 ± 0.02	20.8	99.9
15	MMA/EGMP	Lut. AT 50	150 ± 40	0.91 ± 0.03	22.9	87.3
16	MMA/EGMP	SDS	120 ± 30	1.93 ± 0.04	19.2	96.2

^aS, styrene; MMA, methyl methacrylate; AA, acrylic acid; MA, maleic acid; EGMP, ethylene glycol methacrylate phosphate. ^bDetermined by DLS. ^cDetermined by polyelectrolyte titration. ^dDetermined by TGA.

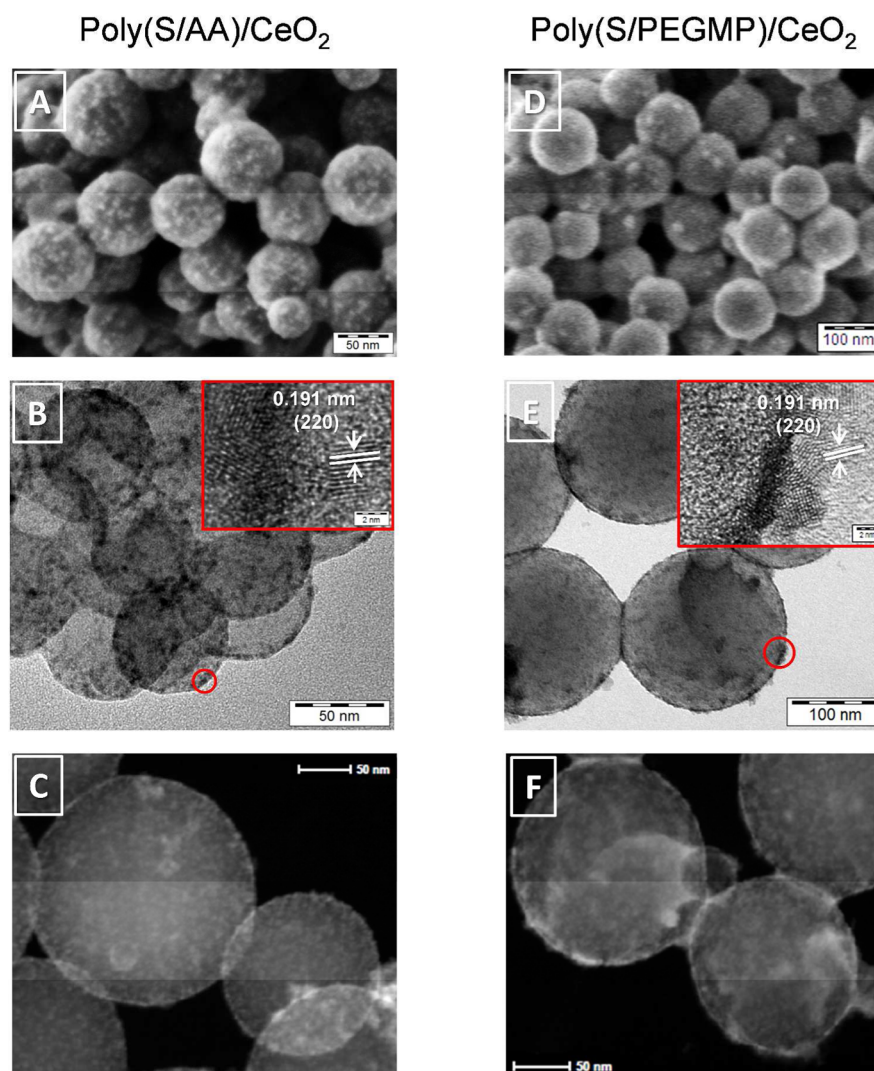


Figure 2. (A) SEM images, (B) TEM images, and (C) dark-field TEM images of CeO_2 /poly(S/AA) hybrid nanoparticles prepared with SDS as a surfactant (sample 4 of Table 1). (D–F) Analogous micrographs for poly(S/EGMP) prepared also with SDS (sample 8 of Table 1). Insets in panels B and E show high-resolution TEM images of selected areas.

(styrene/acrylic acid) and poly(styrene/ethylene glycol methacrylate phosphate) latexes prepared with SDS (samples 4 and 8 of Table 1), are shown in Figure 2. High-resolution TEM micrographs (insets in Figures 2B and 2E) show the presence of crystallites with sizes of 4–5 nm and interplanar spacings of 0.191 nm, which correspond to the (220) crystalline plane for the cubic CeO_2 structure.

X-ray diffraction (XRD) also proved the formation of ceria (JCPDS card No. 34–0394), as shown in Figure 3. The broad reflections indicate a small size of the coherently scattering crystalline domains, typically referred as crystallite size. By applying the Scherrer equation to the reflection (111),⁴⁴ a value of ca. 4 nm was estimated for the crystallites, which is consistent with the TEM observations.

3. Catalyzed Hydration of Nitriles to Amides. The catalytic activity of the CeO_2 /polymer hybrid nanoparticles was tested on the hydration of 2-cyanopyridine to obtain 2-picolinamide (Scheme 1) in a water/ethanol mixture. The product can be easily recovered by washing the catalyst with ethanol and separate it by centrifugation after the conversion is completed. All samples showed very high catalytic efficiency with quantitative yields, typically higher than 95% (Table 1).

Even in the two cases with the lowest surface charge density (latexes prepared with methyl methacrylate and maleic acid or EGMP in the presence of Lutensol AT 50), the reaction yield reached remarkable values of about 87%.

A kinetic study was performed to understand the behavior of the two representative samples whose electron micrographs has been shown in Figure 2. The results indicate that the hydration reaction is complete after 6 to 8 h (Figure 4). The kinetics of the reaction catalyzed with our ceria/polymer hybrid particles is similar as the one of the reaction catalyzed with ceria prepared by bulk precipitation using the same precursor (see the comparison of the kinetics in Figure S3, Supporting Information). Thus, it can be concluded that the polymer supports do not negatively affect the catalytic process. As a reference reference, pure polymer particles without CeO_2 were also tested and they did not show any catalytic effect.

The catalytic particles were shown to be recoverable and even after five cycles there was no significant decrease of the yield, as presented in Figure 5. An important feature of our hybrid particles is that no substantial amount of unreacted product is recovered after washing multiple times the catalyst. Tamura et al.⁴⁵ described in detail the mechanism of the

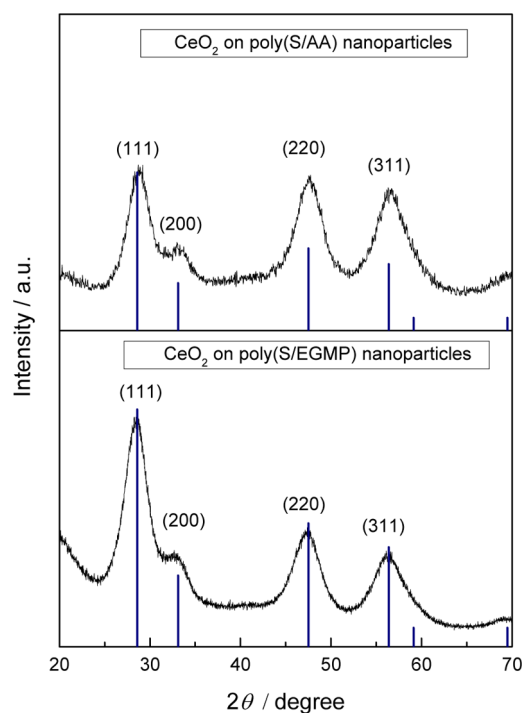


Figure 3. XRD patterns of the representative samples (samples 4 and 8 of Table 1).

Scheme 1. Hydration of 2-Cyanopyridine to 2-Picolinamide

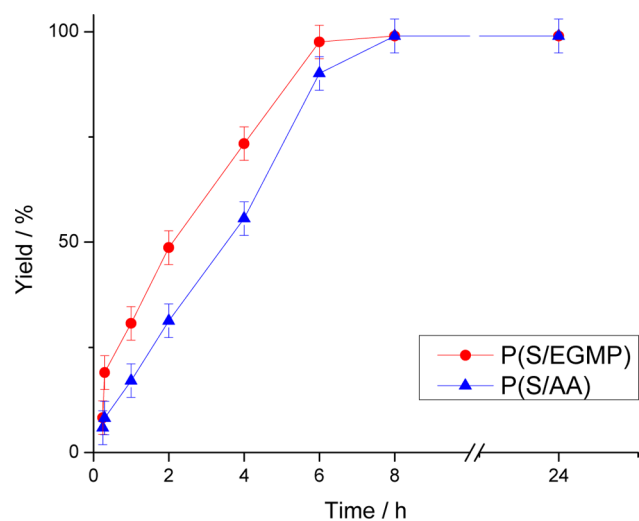
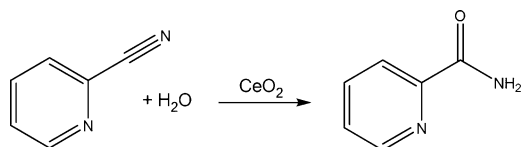


Figure 4. Evolution of the yield with time for the catalytic hydration of 2-cyanopyridine to 2-picolinamide in the presence of samples 4 and 8 (cf. Table 1).

reaction, showing that the substrate is first absorbed on the surface of cerium oxide and then released as a product. In their work, at the end of the reaction the catalyst was washed, and a work up with CHCl_3 followed. From the HPLC experimental observations (Supporting Information, Figure S4), we verified a strong interaction between the catalyst and the substrate, so

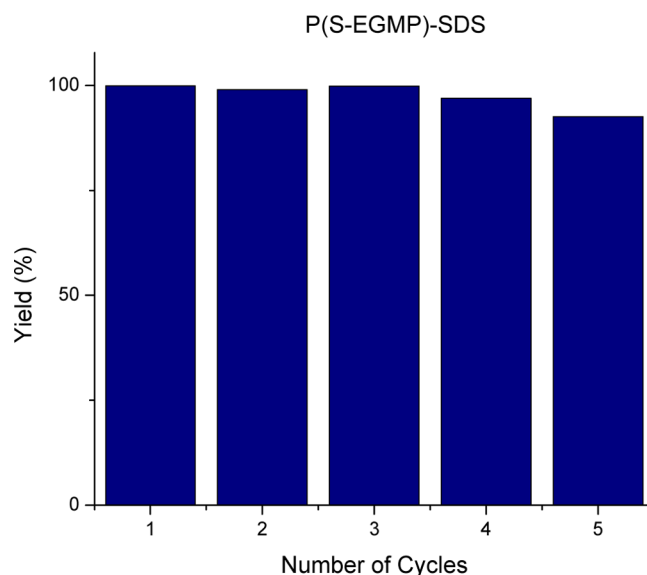


Figure 5. Recyclability of the catalytic particles: yield of the catalytic hydration of 2-cyanopyridine to 2-picolinamide in the presence of sample 8 (cf. Table 1) after several cycles.

that all unreacted fraction remains absorbed on the particles while separating away the product with ethanol. In our case, the workup steps can be minimized, reducing the consumption of solvents and time.

CONCLUSIONS

Hybrid polymer/ CeO_2 nanoparticles were successfully prepared by first synthesizing polystyrene and poly(methyl methacrylate) nanoparticles functionalized on the surface with carboxylic or phosphate groups, and then crystallizing CeO_2 by controlled precipitation from a cerium salt in a basic environment. The combination of two simple techniques gave nanoparticles homogeneously coated with ceria of an average crystallite size of ca. 4 nm. Particles obtained by this procedure are very efficient supported catalysts, as demonstrated for the conversion of 2-cyanopyridine to 2-picolinamide. Quantitative yields were obtained for most of the tested samples, with a high reusability of the without significant decrease in the efficiency. Furthermore, because of the absorption of the substrate to the particle surface, the product can be easily separated without time- and solvent-demanding workup steps.

ASSOCIATED CONTENT

Supporting Information

SEM and TEM images of the different samples, before and after ceria crystallization; yield evolution in the presence of ceria prepared by bulk precipitation from solution; representative example of HPLC curves. The Supporting Information is available free of charge on the ACS Publications website at DOI: 10.1021/acsami.5b01847.

AUTHOR INFORMATION

Corresponding Author

*E-mail: munoz@mpip-mainz.mpg.de. Phone: +49-6131-379-410.

Author Contributions

The manuscript was written through contributions of all authors. All authors have given approval to the final version of the manuscript.

Notes

The authors declare no competing financial interest.

ACKNOWLEDGMENTS

The authors thank Gunnar Glaßer, Katrin Kirchoff, and Michael Steiert for their assistance with SEM, TEM, and XRD, respectively. Beatriz Ma is also acknowledged for her help with BET measurements.

REFERENCES

- (1) Sarkar, S.; Guibal, E.; Quignard, F.; SenGupta, A. K. Polymer-Supported Metals and Metal Oxide Nanoparticles: Synthesis, Characterization, and Applications. *J. Nanopart. Res.* **2012**, *14*, 715.
- (2) Hood, M. A.; Mari, M.; Muñoz-Espí, R. Synthetic Strategies in the Preparation of Polymer/Inorganic Hybrid Nanoparticles. *Materials* **2014**, *7*, 4057–4087.
- (3) Muñoz-Espí, R.; Mastai, Y.; Gross, S.; Landfester, K. Colloidal Systems for Crystallization Processes from Liquid Phase. *CrystEngComm* **2013**, *15*, 2175–2191.
- (4) Wang, X.; Xu, J.; Li, L.; Wu, S.; Chen, Q.; Lu, Y.; Ballauff, M.; Guo, X. Synthesis of Spherical Polyelectrolyte Brushes by Thermo-Controlled Emulsion Polymerization. *Macromol. Rapid Commun.* **2010**, *31*, 1272–1275.
- (5) Schneider, C.; Jusufi, A.; Farina, R.; Li, F.; Pincus, P.; Tirrell, M.; Ballauff, M. Microsurface Potential Measurements: Repulsive Forces between Polyelectrolyte Brushes in the Presence of Multivalent Counterions. *Langmuir* **2008**, *24*, 10612–10615.
- (6) Ballauff, M. Spherical Polyelectrolyte Brushes. *Prog. Polym. Sci.* **2007**, *32*, 1135–1151.
- (7) Ballauff, M.; Borisov, O. Polyelectrolyte Brushes. *Curr. Opin. Colloid Interface Sci.* **2006**, *11*, 316–323.
- (8) Jusufi, A.; Borisov, O.; Ballauff, M. Structure Formation in Polyelectrolytes Induced by Multivalent Ions. *Polymer* **2013**, *54*, 2028–2035.
- (9) Lu, Y.; Mei, Y.; Drechsler, M.; Ballauff, M. Thermosensitive Core-Shell Particles as Carriers for Ag Nanoparticles: Modulating the Catalytic Activity by a Phase Transition in Networks. *Angew. Chem., Int. Ed.* **2006**, *45*, 813–816.
- (10) Lu, Y.; Lunkenbein, T.; Preussner, J.; Proch, S.; Breu, J.; Kempe, R.; Ballauff, M. Composites of Metal Nanoparticles and TiO₂ Immobilized in Spherical Polyelectrolyte Brushes. *Langmuir* **2010**, *26*, 4176–4183.
- (11) Agrawal, M.; Pich, A.; Zafeiropoulos, N. E.; Gupta, S.; Pionteck, J.; Simon, F.; Stamm, M. Polystyrene-ZnO Composite Particles with Controlled Morphology. *Chem. Mater.* **2007**, *19*, 1845–1852.
- (12) Fischer, V.; Lieberwirth, I.; Jakob, G.; Landfester, K.; Muñoz-Espí, R. Metal Oxide/Polymer Hybrid Nanoparticles with Versatile Functionality Prepared by Controlled Surface Crystallization. *Adv. Funct. Mater.* **2013**, *23*, 451–466.
- (13) Agrawal, M.; Pich, A.; Gupta, S.; Zafeiropoulos, N. E.; Formanek, P.; Jehnichen, D.; Stamm, M. Tailored Growth of InOH₃ Shell on Functionalized Polystyrene Beads. *Langmuir* **2010**, *26*, 526–532.
- (14) Bockstaller, M. R.; Mickiewicz, R. A.; Thomas, E. L. Block Copolymer Nanocomposites: Perspectives for Tailored Functional Materials. *Adv. Mater.* **2005**, *17*, 1331–1349.
- (15) Fischer, V.; Bannwarth, M. B.; Jakob, G.; Landfester, K.; Muñoz-Espí, R. Luminescent and Magneto-responsive Multifunctional Chalcogenide/Polymer Hybrid Nanoparticles. *J. Phys. Chem. C* **2013**, *117*, 5999–6005.
- (16) Garnier, J.; Warnant, J.; Lacroix-Desmazes, P.; Dufils, P.-E.; Vinas, J.; van Herk, A. Sulfonated Macro-Raft Agents for the

Surfactant-Free Synthesis of Cerium Oxide-Based Hybrid Latexes. *J. Colloid Interface Sci.* **2013**, *407*, 273–281.

(17) Li, C.; Shu, S.; Chen, R.; Chen, B.; Dong, W. Functionalization of Electrospun Nanofibers of Natural Cotton Cellulose by Cerium Dioxide Nanoparticles for Ultraviolet Protection. *J. Appl. Polym. Sci.* **2013**, *130*, 1524–1529.

(18) Trovarelli, A. Catalytic Properties of Ceria and CeO₂-Containing Materials. *Catal. Rev.-Sci. Eng.* **1996**, *38*, 439–520.

(19) Hegde, M. S.; Madras, G.; Patil, K. C. Noble Metal Ionic Catalysts. *Acc. Chem. Res.* **2009**, *42*, 704–712.

(20) Fernández-García, M.; Martínez-Arias, A.; Iglesias-Juez, A.; Belder, C.; Hungria, A. B.; Conesa, J. C.; Soria, J. Structural Characteristics and Redox Behavior of CeO₂-ZrO₂/Al₂O₃ Supports. *J. Catal.* **2000**, *194*, 385–392.

(21) Reddy, B. M.; Saikia, P.; Bharali, P.; Park, S. E.; Muhler, M.; Grunert, W. Physicochemical Characteristics and Catalytic Activity of Alumina-Supported Nanosized Ceria-Terbium Solid Solutions. *J. Phys. Chem. C* **2009**, *113*, 2452–2462.

(22) Bharali, P.; Thrimurthulu, G.; Katta, L.; Reddy, B. M. Preparation of Highly Dispersed and Thermally Stable Nanosized Cerium-Hafnium Solid Solutions over Silica Surface: Structural and Catalytic Evaluation. *J. Ind. Eng. Chem.* **2012**, *18*, 1128–1135.

(23) Strunk, J.; Vining, W. C.; Bell, A. T. Synthesis of Different CeO₂ Structures on Mesoporous Silica and Characterization of Their Reduction Properties. *J. Phys. Chem. C* **2011**, *115*, 4114–4126.

(24) Reddy, B. M.; Lakshmanan, P.; Loridant, P.; Yamada, Y.; Kobayashi, T.; Lopez-Cartes, C.; Rojas, T. C.; Fernandez, A. Structural Characterization and Oxidative Dehydrogenation Activity of V₂O₅/Ce_xZr_{1-x}O₂/SiO₂ Catalysts. *J. Phys. Chem. B* **2006**, *110*, 9140–9147.

(25) Gonçalves, A.; Silvestre-Albero, J.; Ramos-Fernández, E. V.; Serrano-Ruiz, J. C.; Orfao, J. J. M.; Sepúlveda-Escribano, A.; Pereira, M. F. R. Highly Dispersed Ceria on Activated Carbon for the Catalyzed Ozonation of Organic Pollutants. *Appl. Catal., B* **2012**, *113*, 308–317.

(26) Saceda, J. J. F.; Rintramee, K.; Khabuanchalad, S.; Prayoonpokarach, S.; de Leon, R. L.; Wittayakun, J. Properties of Zeolite Y in Various Forms and Utilization as Catalysts or Supports for Cerium Oxide in Ethanol Oxidation. *J. Ind. Eng. Chem.* **2012**, *18*, 420–424.

(27) Reddy, B. M.; Lakshmanan, P.; Bharali, P.; Saikia, P. Dehydration of 4-Methylpentan-2-ol over Ce_xZr_{1-x}O₂/SiO₂ Nano-Composite Catalyst. *J. Mol. Catal. A: Chem.* **2006**, *258*, 355–360.

(28) Sato, S.; Takahashi, R.; Sodesawa, T.; Honda, N. Dehydration of Diols Catalyzed by CeO₂. *J. Mol. Catal. A: Chem.* **2004**, *221*, 177–183.

(29) Nagashima, O.; Sato, S.; Takahashi, R.; Sodesawa, T. Ketoneformation of Carboxylic Acids over CeO₂-Based Composite Oxides. *J. Mol. Catal. A: Chem.* **2005**, *227*, 231–239.

(30) Gliński, M.; Kijeński, J.; Jakubowski, A. Ketones from Monocarboxylic Acids: Catalytic Ketoneformation over Oxide Systems. *Appl. Catal., A* **1995**, *128*, 209–217.

(31) Abad, A.; Concepción, P.; Corma, A.; García, H. A Collaborative Effect between Gold and a Support Induces the Selective Oxidation of Alcohols. *Angew. Chem., Int. Ed.* **2005**, *44*, 4066–4069.

(32) Yoshida, Y.; Arai, Y.; Kado, S.; Kunimori, K.; Tomishige, K. Direct Synthesis of Organic Carbonates from the Reaction of CO₂ with Methanol and Ethanol over CeO₂ Catalysts. *Catal. Today* **2006**, *115*, 95–101.

(33) Carrettin, S.; Guzmán, J.; Corma, A. Supported Gold Catalyzes the Homocoupling of Phenylboronic Acid with High Conversion and Selectivity. *Angew. Chem., Int. Ed.* **2005**, *44*, 2242–2245.

(34) González-Arellano, C.; Abad, A.; Corma, A.; García, H.; Iglesias, M.; Sánchez, F. Catalysis by Gold(I) and Gold(III): A Parallelism between Homo- and Heterogeneous Catalysts for Copper-Free Sonogashira Cross-Coupling Reactions. *Angew. Chem., Int. Ed.* **2007**, *46*, 1536–1538.

(35) Vivier, L.; Duprez, D. Ceria-Based Solid Catalysts for Organic Chemistry. *ChemSusChem* **2010**, *3*, 654–678.

- (36) Ghaffar, T.; Parkins, A. W. The Catalytic Hydration of Nitriles to Amides Using a Homogeneous Platinum Phosphinito Catalyst. *J. Mol. Catal. A: Chem.* **2000**, *160*, 249–261.
- (37) Cadierno, V.; Francos, J.; Gimeno, J. Selective Ruthenium-Catalyzed Hydration of Nitriles to Amides in Pure Aqueous Medium under Neutral Conditions. *Chem.—Eur. J.* **2008**, *14*, 6601–6605.
- (38) Kim, J. H.; Britten, J.; Chin, J. Kinetics and Mechanism of a Cobalt(III) Complex Catalyzed Hydration of Nitriles. *J. Am. Chem. Soc.* **1993**, *115*, 3618–3622.
- (39) Breno, K. L.; Pluth, M. D.; Tyler, D. R. Organometallic Chemistry in Aqueous Solution. Hydration of Nitriles to Amides Catalyzed by a Water-Soluble Molybdocene, (MeCp)₂Mo(OH)-(H₂O)⁺. *Organometallics* **2003**, *22*, 1203–1211.
- (40) Yamaguchi, K.; Matsushita, M.; Mizuno, N. Efficient Hydration of Nitriles to Amides in Water, Catalyzed by Ruthenium Hydroxide Supported on Alumina. *Angew. Chem., Int. Ed.* **2004**, *43*, 1576–1580.
- (41) Haefele, L. R.; Young, H. J. Catalyzed Hydration of Nitriles to Amides. *Prod. R&D* **1972**, *11*, 364–365.
- (42) Tamura, M.; Wakasugi, H.; Shimizu, K.-i.; Satsuma, A. Efficient and Substrate-Specific Hydration of Nitriles to Amides in Water by Using a CeO₂ Catalyst. *Chem.—Eur. J.* **2011**, *17*, 11428–11431.
- (43) Muñoz-Espí, R.; Qi, Y.; Lieberwirth, I.; Gómez, C. M.; Wegner, G. Surface-Functionalized Latex Particles as Controlling Agents for the Mineralization of Zinc Oxide in Aqueous Medium. *Chem.—Eur. J.* **2006**, *12*, 118–129.
- (44) Klug, H. P.; Alexander, L. E. *X-ray Diffraction Procedures for Polycrystalline and Amorphous Materials*, 2nd ed.; John Wiley: New York, 1974.
- (45) Tamura, M.; Satsuma, A.; Shimizu, K.-i. CeO₂-Catalyzed Nitrile Hydration to Amide: Reaction Mechanism and Active Sites. *Catal. Sci. Technol.* **2013**, *3*, 1386–1393.